SURVEY OF RESULTS IN THE A=70 TO 80 REGION*

JÜRG X. SALADIN

Department of Physics and Astronomy, University of Pittsburgh
Pittsburgh, PA 15260, USA

1. Introduction

High spin phenomena in the A=70 to 80 region differ in unique ways from those in the rare earth and in the actinide region. In the A=70 to 80 region, neutrons and protons fill the same orbitals and, more importantly, the same unique parity g9/2 intruder states. The level density in this region is furthermore only about one half that of the rare earth region and the shells are smaller. As a result of these properties, pairing correlations are weaker and more easily quenched under the influence of the Coriolis interaction and/or as a result of changes in configurations. For the same reasons one expects, and finds in this region, rapid structural changes as a function of angular momentum and as a function of the neutron number N and the proton number Z. These structural changes manifest themselves as changes in shape, by the occurrence of shape coexistence, changes in the moments of inertia $\Im$ and in crossing frequencies ω_c. These effects can be understood in terms of an interplay between deformation driving forces, pairing correlations and the Coriolis interaction.

Nilsson diagrams for neutrons and protons calculated with the Warsaw Potential[1] are shown in Figs. 1 and 2. For both protons and neutrons, one observes near-spherical or prolate shell gaps competing with oblate shell gaps for N or Z=34 and 36. Highly prolate gaps are predicted for N or Z=38, while for N or Z=40, there are several gaps covering the deformation region from β_2= -.35 to +.45 including nearly spherical shapes. Hence, for certain combinations of Z and N, the neutrons tend to prefer prolate deformations while the protons prefer oblate shapes.

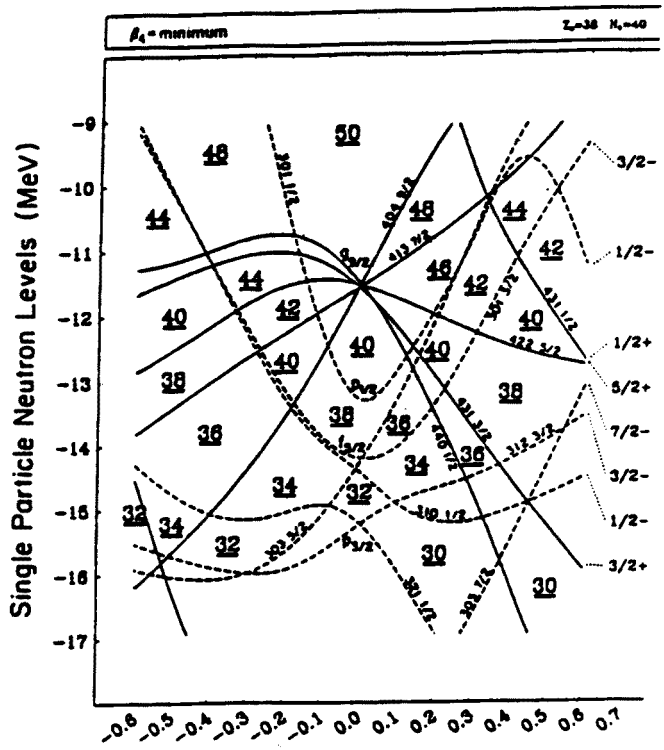

Fig. 1.

* Received post deadline

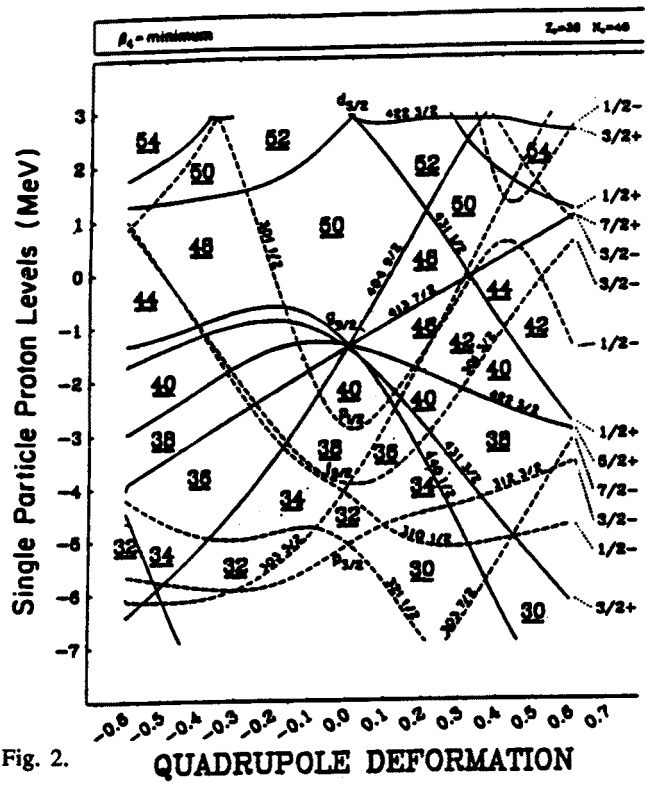

Fig. 2.

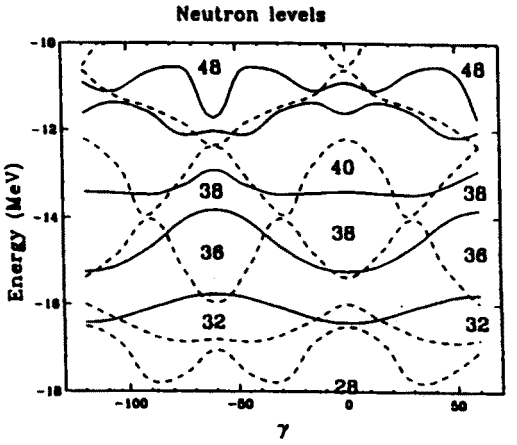

Fig. 3. Nilsson orbitals as a function of γ for β_2=0.38.

This competition can lead to nuclei which exhibit coexisting prolate and oblate states or which are γ-soft. At higher spins, γ-soft nuclei may develop stable triaxial deformations. The strong dependence of the Nilsson orbitals for neutrons on the γ-degree of freedom is illustrated in Fig. 3. The results for protons are nearly identical except for an overall shift in energy.

Fig. 4 shows total Routhian surfaces for several even-even nuclei at angular frequencies of $\hbar\omega$=0.2 and 0.8 MeV, i.e., before and after the first backbend. They are the results of cranked Wood-Saxon-Bogoliubov calculations with Strutinsky averaging (CWSBS)[2,3,4]. Pairing was treated self consistently at both values of ω. At $\hbar\omega$=0.2 MeV, ^{74,76,78}Kr show coexisting collective prolate and oblate minima. However, the surfaces are quite soft in the γ-degree of freedom. The TRS's of ^{72,74}Se are even softer and only a collective (and non-collective) oblate minimum is recognizable. It should be noted that relatively low lying 0_2+ states (between 854 and 1122 keV) have been observed[5] in all of these nuclei except ^{74}Kr. At $\hbar\omega$=0.8 MeV after the proton and neutron alignment, the lowest minima in ^{74,76}Kr and ^{72}Se correspond to prolate deformations with a small, positive γ. ^{74}Se has two rather distinct collective and non-collective triaxial minima and ^{78}Kr seems to prefer an oblate shape.

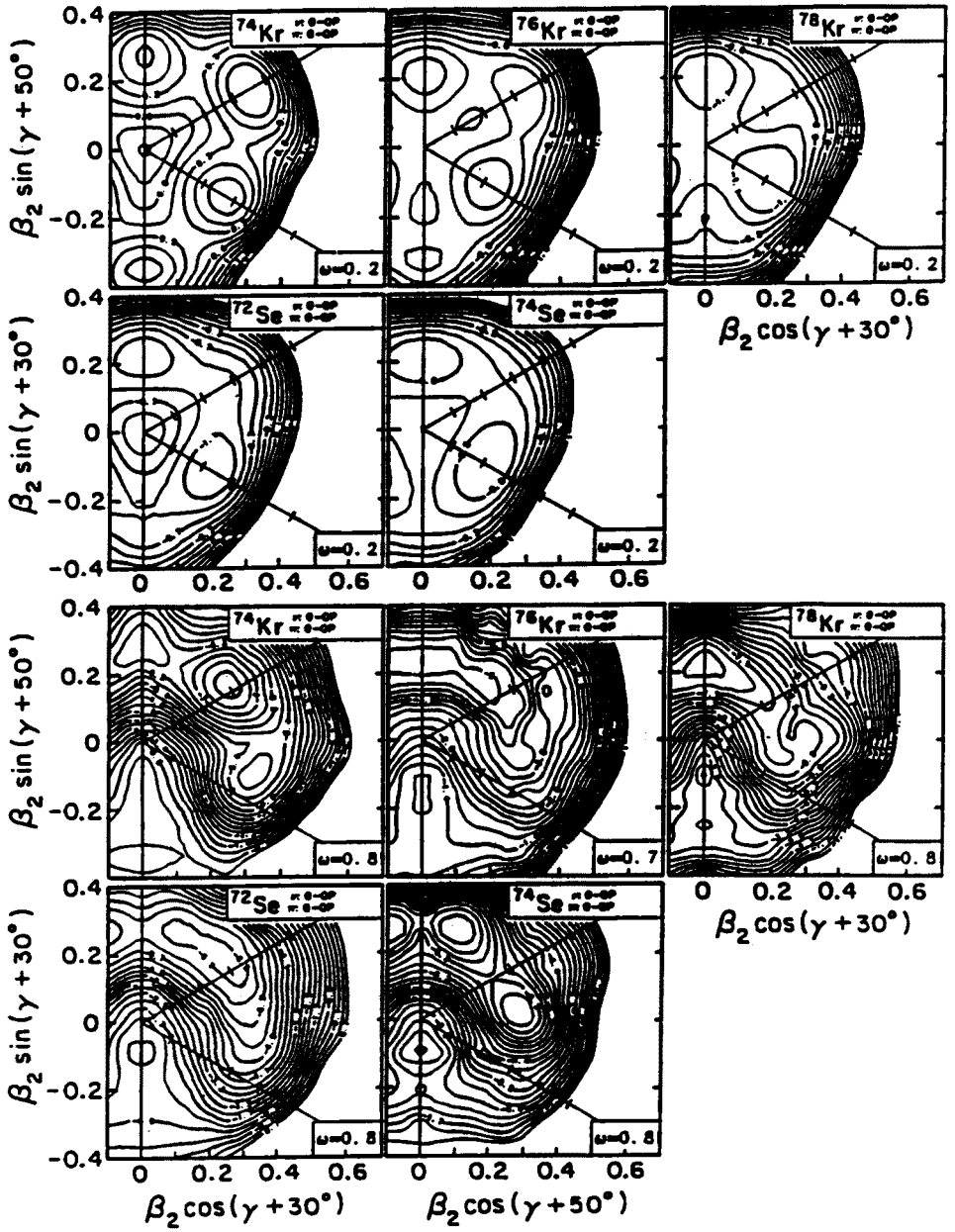

Fig. 4. Total Routhian surfaces for several nuclei for $\hbar\omega$=0.2 and 0.8 MeV. Pairing was treated self-consistently at all values of ω.

In the following, some of the features of high spin phenomena in the A=70 to 80 region are discussed by way of some typical examples.

2. Band Structure in Even-Even Nuclei

Fig. 5 shows the aligned angular momenta i for three even-even nuclei that are representative for this region, namely $^{74,76,78}Kr$[6,7,8,9]. The alignment is given relative to the negative parity even spin band in ^{76}Kr which behaves like a very good rigid rotor. Of particular interest is the marked difference in the alignment pattern of ^{78}Kr compared to that of $^{74,76}Kr$. The latter two isotopes exhibit a single upbend at $\hbar\omega$= 0.67 MeV with a large alignment Δi=0.6 while ^{78}Kr displays two distinct alignments at $\hbar\omega$=0.56 MeV and at $\hbar\omega$=0.9 MeV with Δi=3.8 and 2.2, respectively. The sum of the two alignments in ^{78}Kr equals that of the single alignment in $^{74,76}Kr$. This suggests that the proton and neutron alignments in $^{74,76}Kr$ occur within 10 to 20 keV of one another, while in ^{78}Kr, one of the two alignments is significantly delayed (i.e., by about 320 keV). Systematics of even-odd and odd-even Kr,Se and Rb nuclei suggest that the first upbend in $^{74,76}Kr$ is due to proton alignment and that the neutron upbend should occur about 50 to 100 keV later. The almost simultaneous alignments of protons and neutrons has been studied by Nazarewicz[9] by means of cranked Wood-Saxon-Bogoliubov calculations which showed that the nuclear shape changes during the first proton alignment, and that it is this shape change which pushes the neutron crossing frequency down to within ~10 keV of the proton crossing. Fig. 6 shows total Routhian surfaces for ^{76}Kr as a function of ω illustrating the change in deformation parameters from β,γ=0.36, -5.5° before the upbend, to β,γ=0.25, +16° after the upbend. Fig. 7 summarizes the shape changes as a function of $\hbar\omega$ for $^{74,76,78}Kr$. One notes in all three isotopes a significant "shrinking" of β_2 during the upbend. In Fig. 8, the experimental kinematic moment of inertia of ^{76}Kr is compared with the results of cranking calculations. The latter represent the data quite well. The decomposition into the contributions from neutrons and protons illustrates the nearly simultaneous alignments. The proton alignment comes first (as anticipated) and is fairly rapid, while the neutron alignment is more gradual.

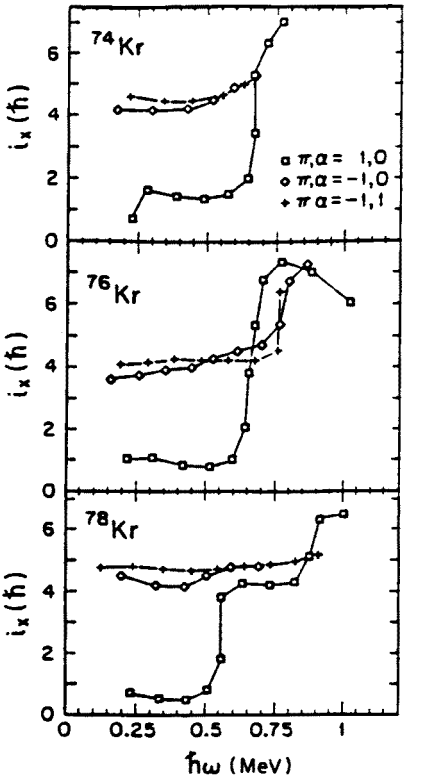

Fig. 5. Alignment plots for $^{74,76,78}Kr$.

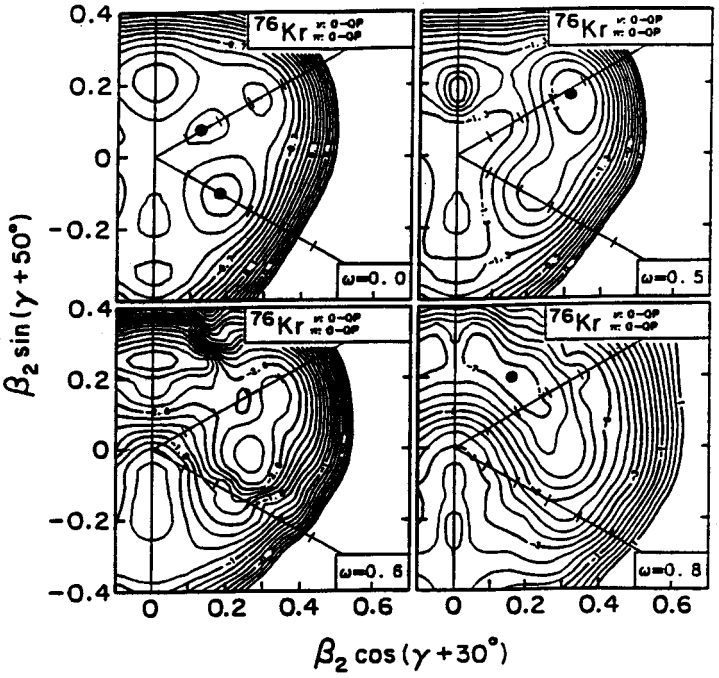

Fig. 6 Total Routhian surfaces for ^{76}Kr for $\hbar\omega$=0.0, 0.5, 0.6 and 0.8 MeV. Full circles indicate the positions of the lowest minima

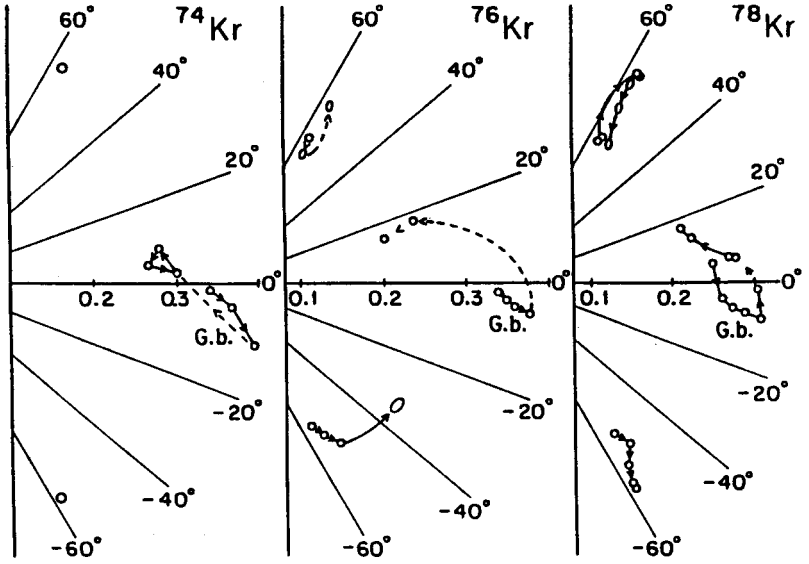

Fig. 7. Deformation paths in the β-γ plane as a function of ω for several minima in the TRS surfaces of ^{74,76,78}Kr. The arrows indicate the direction of increasing ω.

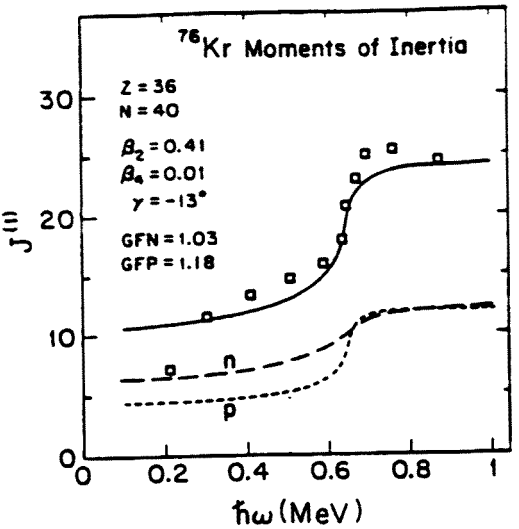

Fig. 8. Experimental and calculated moments of inertia for ^{76}Kr. The contributions due to neutrons and protons are labeled n and p, respectively.

Fig. 9 shows the quasiparticle Routhians for ^{78}Kr for β,γ=.36, 21°. It predicts the proton alignment at the correct frequency but cannot account for delays in the neutron alignment.

A summary of experimental crossing frequencies for the positive parity positive signature band of nuclei in this region is presented in Fig 10. The neutron crossing frequency of ^{78}Kr clearly does not fit into this systematic. This puzzle has only recently been cleared up by Billowes et al.[10,11] who determined the g-factor in the region of the first upbend in ^{78}Kr. They found a considerable drop in the g-factor at spin 8^+ compared to the g-factors of the lower spin states. This is strong evidence that in ^{78}Kr, the first upbend is in fact due to neutron alignment. In earlier work Nazarewicz[9] investigated the qualitative features of the shape dependence of the crossing frequencies of the even Kr isotopes by means of schematic cranked Wood-Saxon-Bogoliubov (CWSB) calculations in which the pairing gap was kept constant. These results are summarized in Fig. 11. The left panel is for axially symmetric prolate shapes while the right panel shows the result of axially symmetric oblate shapes.

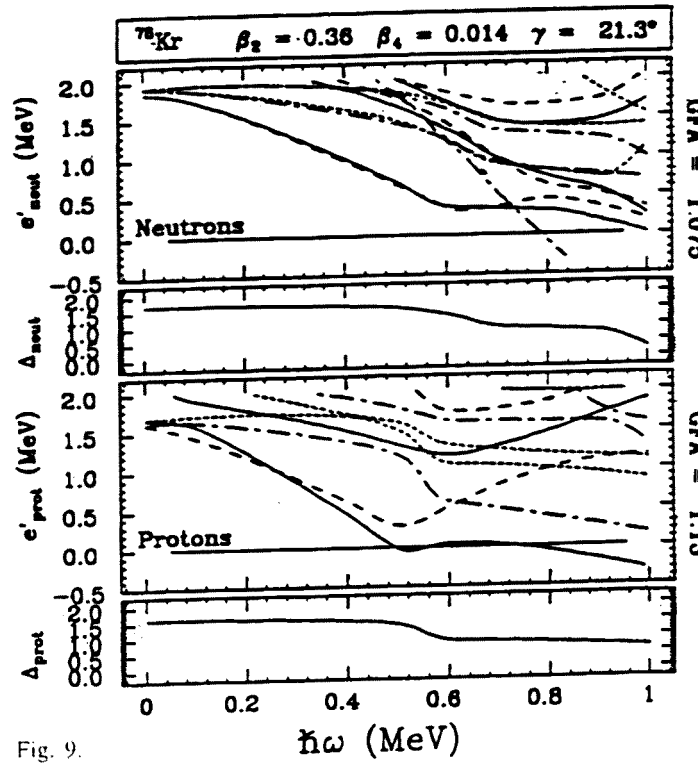

Fig. 9.

The right panel thus indicates that for an oblate shape, the neutron crossing indeed takes place first and is followed about 300 keV later by a proton crossing.

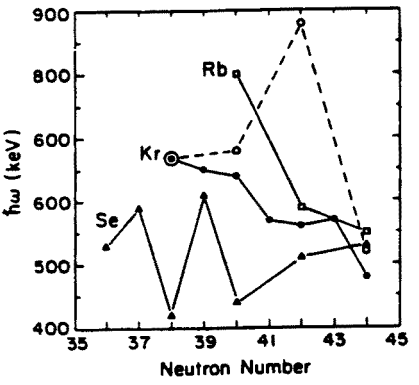

Fig. 10. Systematics of experimental crossing frequencies for the positive parity, positive signature bands in Se, Kr and Rb. Open symbols represent neutron crossings. Filled symbols are for proton crossings.

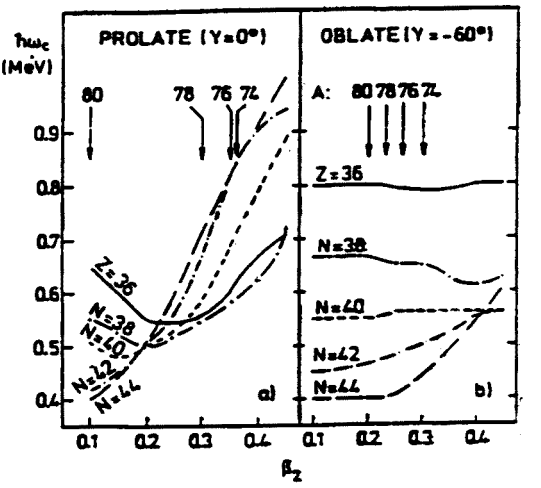

Fig. 11. Bandcrossing frequencies $\hbar\omega_0$ for protons (Z=36) and for neutrons (N=38 to 44) as a function of β_2. The left (right) panel is for prolate (oblate) shapes.

The TRS surfaces shown in Fig. 12 clearly indicate that, at least before the upbend, the oblate minimum is indeed lower in energy. Thus, we see here a very dramatic shape transition from collective prolate to collective oblate due to the addition of two neutrons. It is important to note here that the investigation of the sequence of, and the separation between, proton and neutron crossings provides a powerful tool for differentiating between prolate and oblate shapes.

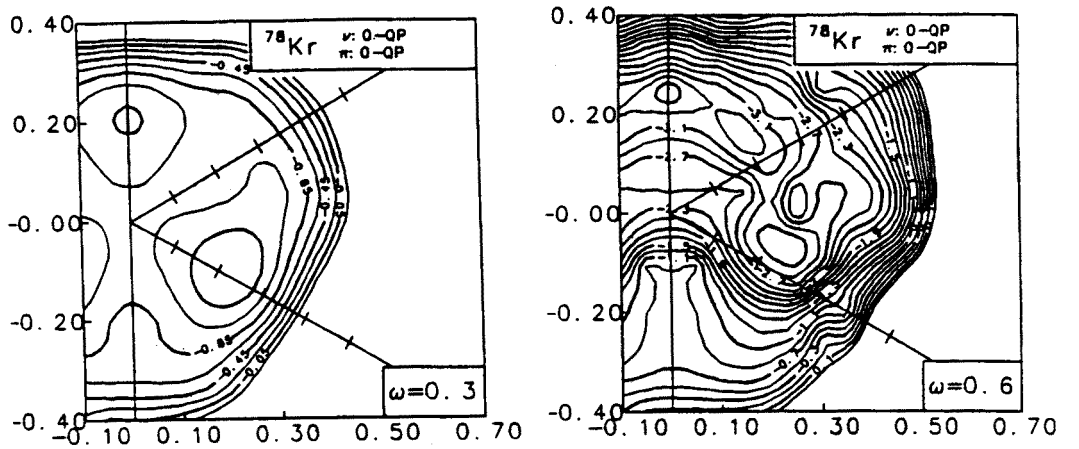

Fig. 12. Total Routhian surfaces for ^{78}Kr before and after the first upbend.

3. Odd N Nuclei

It is interesting to study the effects associated with the addition of an odd nucleon to an even-even core. In the following discussion we use as examples the two recently investigated nuclei, ^{73,75}Se[12,13]. The coexistence of well deformed prolate and oblate shapes in the neighbouring even-even nuclei ^{72,74}Se is experimentally well established[14,15]. In some cases, such as ^{73}Br, the odd nucleon (proton in this case) has been found to polarize the core, thus stabilizing one of the shapes[16,17,18,19] and quenching shape coexistence. Figs. 13 and 14 show the level schemes for the positive and negative parity bands in ^{73,75}Se.

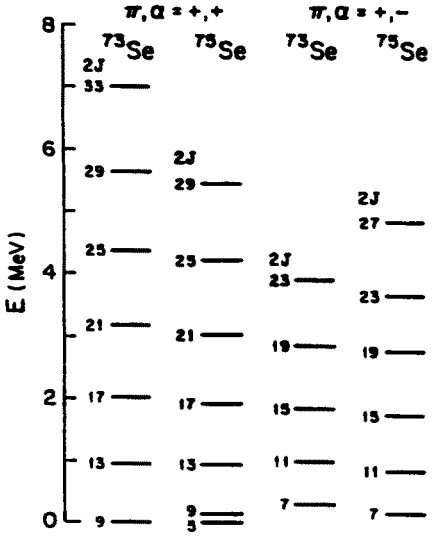

F.g. 13. Level schemes of ^{73,75}Se for the positive parity band.

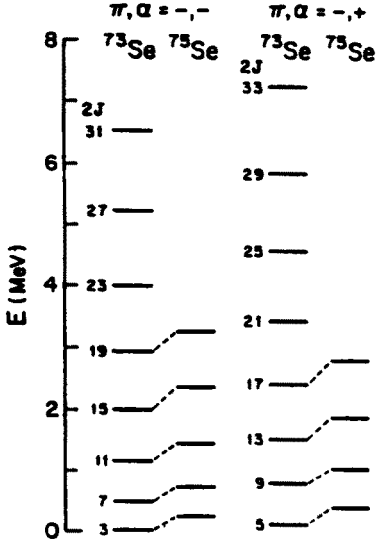

Fig. 14. Level schemes of ^{73,75}Se for the negative parity band.

It should be noted that the positive parity yrast band in ^{73}Se is built on the 9/2+ ground state, while that of ^{75}Se is based on a 5/2+ ground state. Experimental Routhians are shown in Fig. 15. The negative parity bands in ^{73}Se show very little signature splitting up to the highest spins observed, typical for the strongly coupled negative parity bands observed in neighbouring isotopes[20,21,22,23]. The corresponding signature splitting in ^{75}Se is somewhat larger, ranging from 80 keV at $\hbar\omega$=.2 MeV, to 160 keV at $\hbar\omega$=.4 MeV. The positive parity bands, by contrast, display very large signature splittings which decrease with increasing $\hbar\omega$. Plots of the kinematic momenta of inertia $\mathcal{I}^{(1)}$ and the alignment i versus $\hbar\omega$ are shown in Fig. 16. In both nuclei, the $\mathcal{I}^{(1)}$ and i rise rapidly for the π,α=+,- unfavoured configuration while the rise is somewhat more gradual for the favoured signature bands (π,α=+,+). A similar strong configuration dependent alignment has recently been observed in ^{73}Rb[24]. These signature dependent alignments reflect signature dependent interactions between crossing bands. This has also been observed in rare earth nuclei[25].

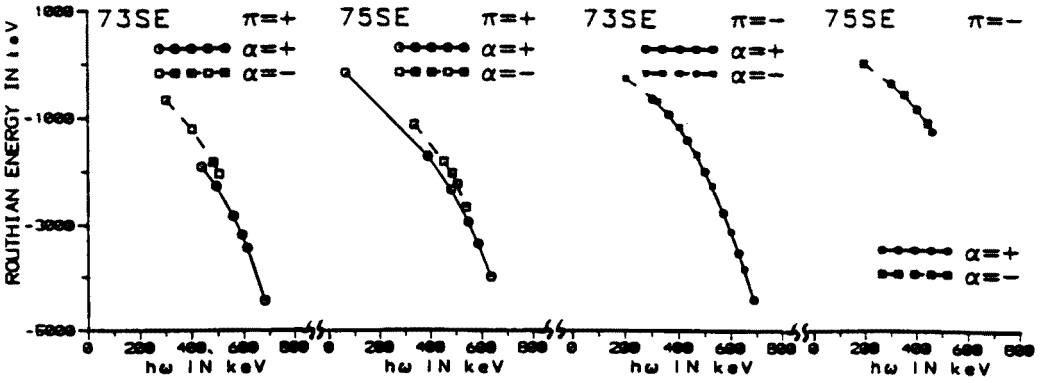

Fig. 15. Experimental Routhians for ^{73,75}Se for the positive parity band.

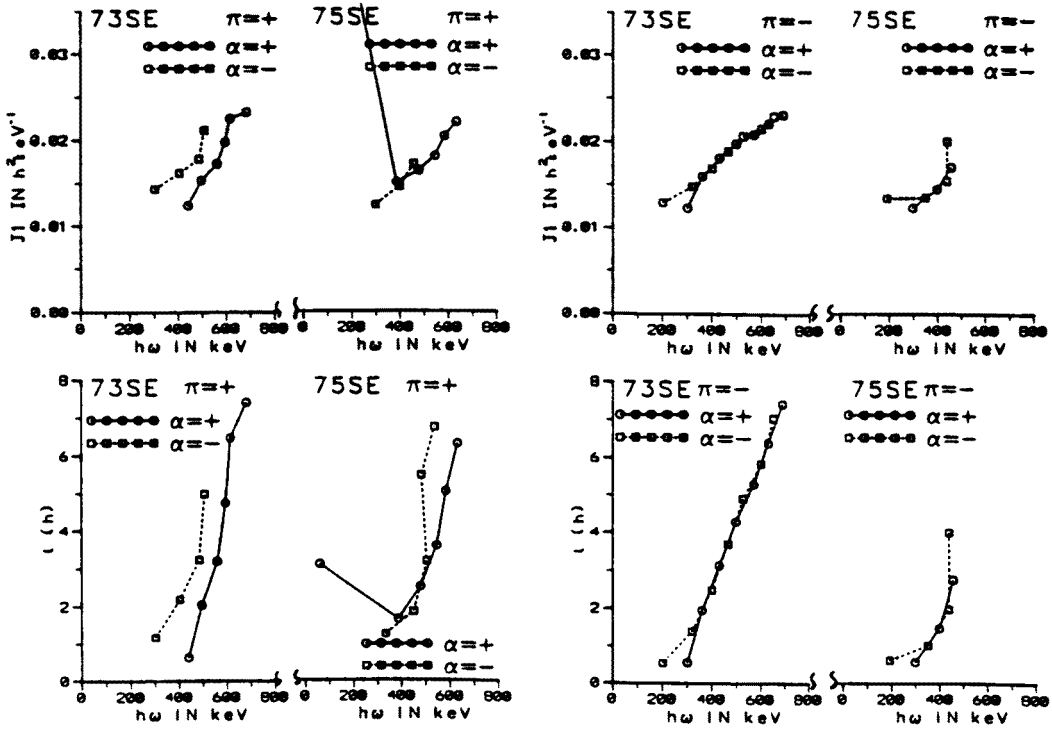

Fig. 16a. $\mathcal{I}^{(1)}(\omega)$ and $i(\omega)$ for ^{73,75}Se.

Fig. 16b. $\mathcal{I}^{(1)}(\omega)$ and $i(\omega)$ for ^{73,75}Se.

The corresponding plots for the negative parity sequences, on the other hand, indicate good rotational behaviour. This is particularly true for ^{73}Se.

For the positive parity bands, the Nilsson diagram (Fig. 1) associates axially symmetric prolate shapes with the 422 5/2+ orbital and axially symmetric oblate shapes with the 404 9/2+ orbital. However, strong mixing among the g9/2 orbitals is expected for γ-soft or triaxial or near-spherical shapes. The difference in the ground state spins of ^{73}Se and ^{75}Se suggests rather different admixtures from among the g9/2 orbitals.

Another possibility is that the ground state bands are decoupled bands built on an even-even core. The results of a least square fit to the positive parity energy levels in ^{73}Se using the expression

$$E = A\, I(I+1) + A_1\, (-1)^{I+\frac{1}{2}}(I+\tfrac{1}{2})$$

for decoupled bands is shown in Fig. 17. The discrepancy between the fit and the data for the lower numbers of the band might be an indication of shape coexistence between rotational and vibrational structures. In Fig. 18 the positive parity bands of ^{73,75}Se are compared to the ground state bands of ^{72,74}Se. It can be seen that the level spacing between the α=+1/2 states are comparable to the spacings found in the even-even nuclei. This suggests that the ground state bands in ^{73,75}Se are decoupled.

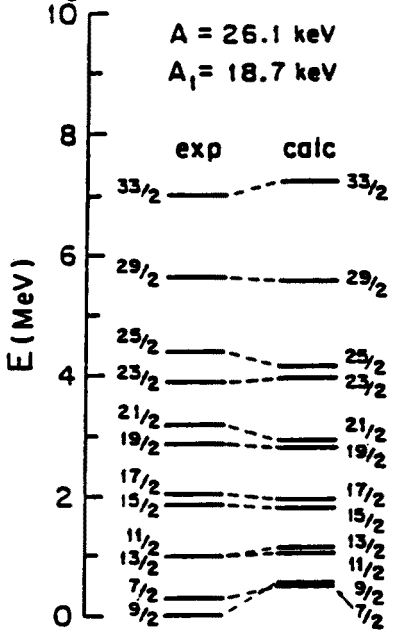

Fig. 17. Comparison of experimental levels to the results of a fit using the decoupled band expression. (See text.)

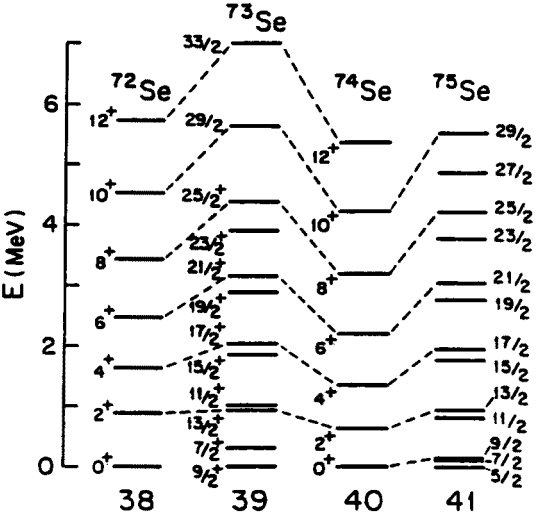

Fig. 18. Comparison of the level schemes of ^{73,75}Se with the neighbouring even-even nuclei ^{72,74}Se.

The large signature splitting observed in the positive parity bands points to a strong influence associated with the γ-degree of freedom. Collective bands built on high Ω orbitals in well deformed, axially symmetric nuclei should be subject to little mixing with the Ω=1/2 orbital responsible for signature splitting.

3a. Interpretation

Fig. 19 shows total Routhian surfaces for both isotopes below and above the region of the proton upbend. A general feature of these surfaces is the considerable degree of γ-softness and the existence of multiple minima. The shape evolutions of ^{73}Se and ^{75}Se are quite different. In ^{73}Se, the two signature partners are, at $\hbar\omega$=3 MeV, very similar in shape and approximately axially symmetric. After the proton alignment at $\hbar\omega\simeq$6 MeV, the π=+,+ band prefers a noncollective triaxial shape, while the π,α=+,- band remains nearly axially symmetric. Both surfaces are however, very γ-soft.

In ^{75}Se, the shapes of the two positive parity signature partners differ already at $\hbar\omega$=.3 MeV. The π,α=+,+ band prefers a collective triaxial shape while the π,α=+,- band prefers a nearly axially symmetric collective oblate shape. At $\hbar\omega$=0.6 MeV, the π,α=+,+ band remains collectively triaxial, while the π,α=+,- band prefers a noncollective triaxial shape. The shape driving forces in the γ-degree of freedom are illustrated in Fig. 20, which is a plot of one-quasi neutron Routhians (from Ref. 13) for ^{75}Se(N=41) as a function of γ. One observes a large signature splitting for the lowest positive parity Routhians for $\gamma<0$; the positive signature partner (solid curve) has a minimum at $\gamma\sim$-40°, while the negative signature partner is nearly independent of γ.

The calculated proton and neutron alignments I_x for both nuclei and for both signature partners of the positive parity bands are shown in Fig. 21. The labels on the arrows indicate the triaxiality parameter γ. In ^{75}Se it is the large collective triaxiality ($\gamma<0$) which leads to the large signature splitting, (see Fig. 20.) Fig. 21 shows that the proton alignment does not change the triaxiality of the favoured band significantly, but the proton alignment is followed by a neutron alignment which drives the nucleus to non-collective triaxiality ($\gamma>0$).

The triaxiality of the unfavoured band is very γ-soft at low $\hbar\omega$ and the proton alignment leads immediately to a shape transition from collective to non-collective triaxiality. This shape change results in a reduction in signature splitting in agreement with Fig. 20 and with experiment.

In ^{73}Se, the situation is somewhat different. For $\hbar\omega\lesssim$.4 MeV, the shapes of the two signature partners are nearly identical and nearly axially symmetric. After the proton and neutron alignment, the favoured band assumes a non-collective triaxial shape. The unfavoured band remains very γ-soft with a near axially symmetric minimum which coexists with a minimum at $\gamma\sim$+35° which is only ~60 keV higher in excitation energies. The calculations predict a significant amount of signature splitting for $\hbar\omega>$.3 MeV in agreement with experiment.

The negative parity bands in the two isotopes ^{73,75}Se behave very similar. Below the proton alignment at $\hbar\omega$=.3 MeV, the deformation for both signature partners is $\beta,\gamma\simeq$.32, -10°. After the upbend, the shape becomes at $\hbar\omega$=.6 MeV, as a result of the proton alignment non-collective triaxial, with $\beta,\gamma\simeq$.3, + 30°. The signature splitting is predicted to be small, in agreement with the data.

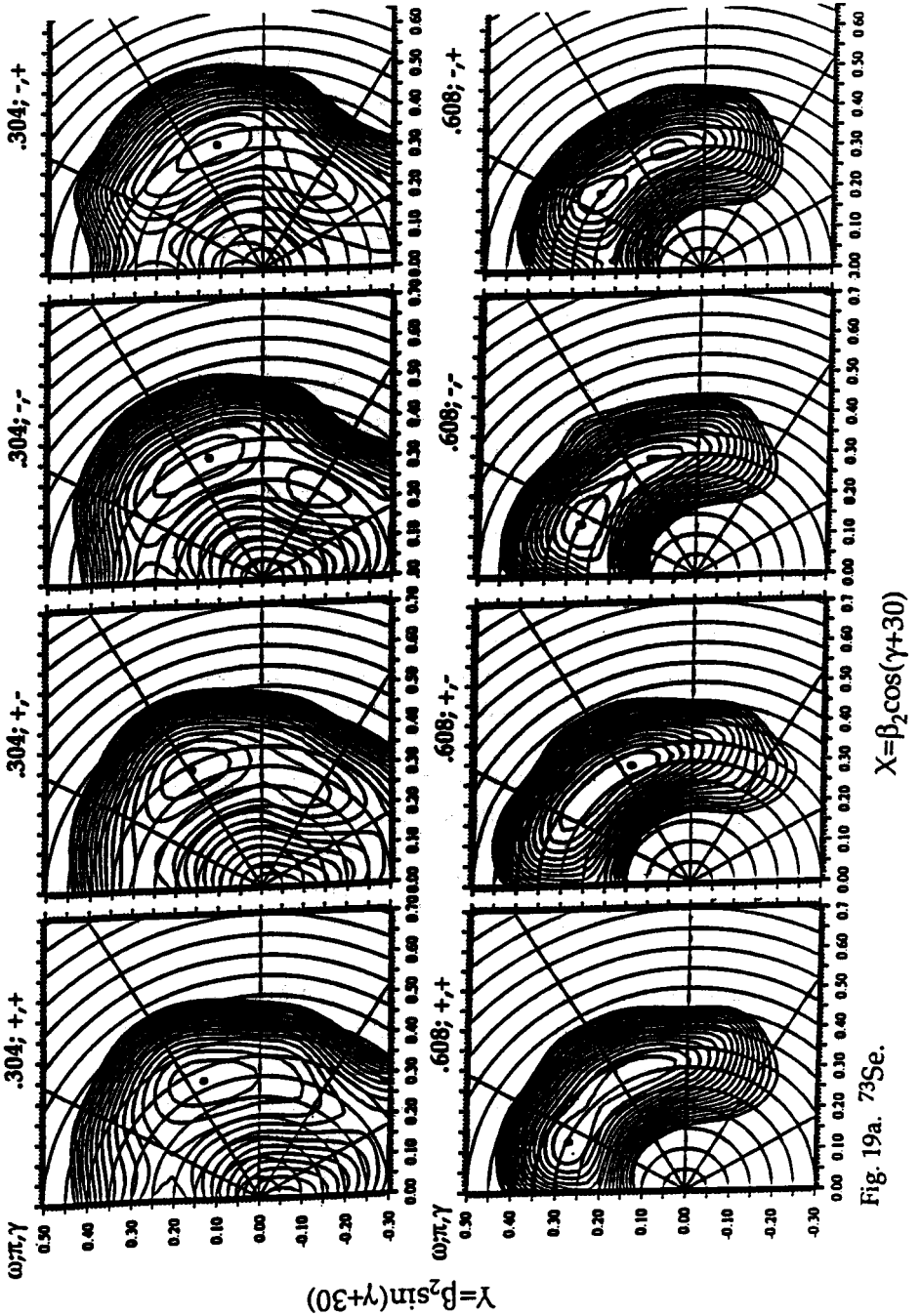

Fig. 19a. ^{73}Se.

Fig. 19a(19b). Total Routhian surfaces (from Nazarewicz data base) for ^{73}Se(^{75}Se). The labels on top of each graph indicate $\hbar\omega$ in MeV and the parity π and signature α.

Fig. 19b. ^{73}Se.

Fig. 19b

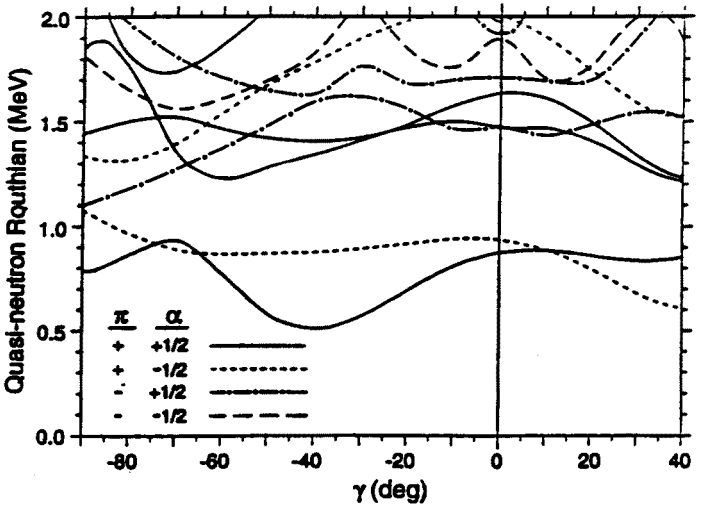

Fig. 20. Quasineutron Routhians for ^{75}Se as a function of γ. β_2=.28 $\hbar\omega$=0.3 MeV. (From Ref. 13.)

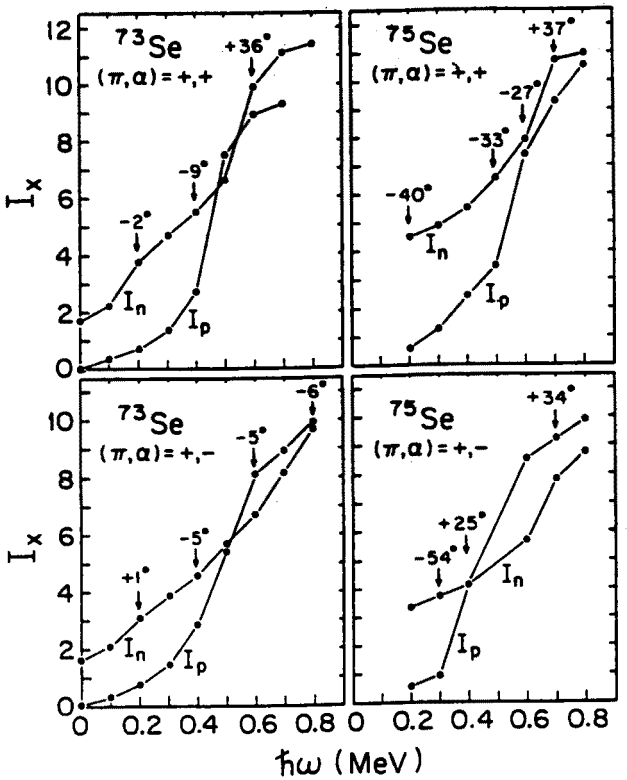

Fig. 21. Calculated neutron and proton alignments for ^{73,75}Se. The labels on the points indicate the values of the triaxiality parameter γ at the corresponding minimum. (Extracted from the Nazarewicz data base.)

Summary

The systematics of the band crossings in the Kr isotopes was discussed and compared with the predictions from cranked Wood-Saxon-Bogoliubov calculations. A longstanding puzzle concerning the high neutron crossing frequency in ^{78}Kr seems to have been resolved by recent g-factor measurements of the Daresbury group which indictes that the ground band of ^{78}Kr has an oblate shape.

The alignment patterns of the positive parity bands in ^{73}Se and ^{75}Se are compared. It is seen that the shape evolution as a function of the rotational frequency ω is, in both nuclei, strongly signature dependent.

Acknowledgements:

Stimulating discussions with W. Nazarewicz, J. Dudek, J. Heese and F. Cristanco are gratefully acknowledged. Part of this work was supported by a grant from the US National Science Foundation.

References

1. S. Cwiok et al., Comp. Phys. Comm **46** 379 (1987).
2. R. Bengtsson and S. Frauendorf, Nucl. Phys. **A327** 139 (1979).
3. R. Bengtsson and S. Frauendorf, Nucl. Phys. **A314** 27 (1979).
4. Nazarewicz et al., Nucl. Phys. **A435** 397 (1985).
5. See e.g., Nucl. Data Sheets.
6. S.L. Tabor et al., Phys. Rev. **C41** 2658 (1990).
7. J. Heese et al., Phys. Rev. **C43** R921 (1991).
8. M.S. Kaplan et al., Phys. Lett **B215**, 251 (1988).
9. C.J. Gross et al., Nucl. Phys. **A501** (1989).
10. J. Heese, Private communication.
11. Billowes et al., Preprint.
12. M.S. Kaplan et al., Phys. Rev. **C44** 668 (1991).
13. T.D. Johnson et al., Phys. Rev. **C46** 516 (1990).
14. J.H. Hamilton et al., Phys. Rev. Lett **36** 340 (1976).
15. R.B. Piercey et al., Phys. Rev **C25** 1941 (1982).
16. J. Heese et al., Phys. Rev. **C36** 2409 (1987).
17. B. Wörmann et al., Z Phys. **A322** 171 (1985).
18. L. Lühmann et al., Phys. Rev. **C31** 828 (1985).
19. L. Lühmann et al., Europhys. Lett. Z 623 (1986).
20. K.O. Zell et al., Z. Phys. **A279** 373 (1976).
21. A. Dewald et al., Z. Phys. **A326** 508 (1987).
22. G. Garcia et al., Phys. Rev. **C30** 43 (1987).
23. D.F. Winchell et al., Phys Rev. **C40** 2672 (1989).
24. Skeppstedt et al., Nucl. Phys. **A511** 137 (1990).
25. G. Hagemann and I. Hamamoto, Phys. Rev. **C46** 838 (1992).